C. R. Chimie 17 (2014) 534–540

Contents lists available at ScienceDirect

Comptes Rendus Chimie

www.sciencedirect.com

Full paper/Mémoire

Application of the infrared spectroscopy to the structural study of Prussian blue analogues

Julien Lejeune [a,*], Jean-Blaise Brubach [b], Pascale Roy [a,b], Anne Bleuzen [a]

[a] Institut de chimie moléculaire et des matériaux d'Orsay, UMR CNRS 8182, Université Paris-Sud, 15, rue Georges Clémenceau, 91405 Orsay cedex, France
[b] Synchrotron SOLEIL, L'Orme des Merisiers Saint-Aubin, BP 48, 91192 Gif-sur-Yvette cedex, France

ARTICLE INFO

Article history:
Received 22 August 2013
Accepted after revision 20 January 2014
Available online 13 March 2014

Keywords:
Prussian blue analogues
Infrared spectroscopy
Alkali-cyanide interaction
Metal–ligand bonds
Switchable compounds

Mots clés :
Analogues du bleu de Prusse
Spectroscopie infrarouge
Interaction alcalin–cyanure
Liaisons métal–ligand
Composés commutables

ABSTRACT

Prussian blue analogues (PBAs) form a versatile family of inorganic polymers that may exhibit promising electronic and magnetic properties. Owing to the partially disordered structure of these systems, a comprehensive characterization of PBAs is often tricky and requires the use of numerous complementary techniques. We present herein an original use of infrared (IR) spectroscopy in the characterization of PBAs. Based on a detailed assignment of both the far- and mid-IR spectra of PBAs, including the description of the metal–ligand bonds and the water molecules in PBAs, we demonstrate that IR spectroscopy allows investigating the electronic and structural properties of PBAs.

RÉSUMÉ

Les analogues du bleu de Prusse (ABP) constituent une famille de polymères inorganiques particulièrement versatiles, pouvant présenter des propriétés électroniques et magnétiques prometteuses. En raison de la nature partiellement désordonnée de ces systèmes, une caractérisation complète des ABP est la plupart du temps difficile et nécessite la mise en jeu de nombreuses techniques complémentaires. Nous présentons dans cet article une approche originale de la caractérisation des ABP par spectroscopie infrarouge (IR). Grâce à l'attribution détaillée des spectres des ABP dans les lointain et moyen IR, incluant une description des bandes de vibration métal–ligand et des molécules d'eau au sein des ABP, nous démontrons ici la pertinence de la spectroscopie IR dans l'étude des propriétés électroniques et structurales des ABP.

1. Introduction

Prussian blue analogues (PBAs) form a wide class of inorganic polymers exhibiting numerous appealing electronic and chemical properties, including room-temperature magnetic properties [1,2], large porous volumes (suitable for gas storage applications) [3–5], electrochemical properties for alkali cation-based batteries [6,7], and electronically switchable properties [8–10]. The understanding of the physical and chemical phenomena occurring at the atomic scale in PBAs is needed to finely tune up these promising properties. Infrared (IR) spectroscopy has recently been evidenced as a well-adapted probe of the electronic and structural properties of PBAs at the molecular level [11]. However, no comprehensive assignment of the IR spectrum of PBAs was available—to date—in the literature.

We demonstrate herein the relevance of the IR approach to the probing of the electronic and structural properties of PBAs. A comprehensive assignment of the IR spectrum of PBAs is performed based on the electronically switchable

* Corresponding author.
E-mail address: julien.lejeune@ens-lyon.org (J. Lejeune).

1631-0748/$ – see front matter
http://dx.doi.org/10.1016/j.crci.2014.01.017

series of cobalt–iron PBAs [12,13]. Both the far-IR region and the spectral range associated with the ν{O–H} of the water molecules of PBAs are discussed. Using these assignments, examples of the use of IR spectroscopy as an accurate tool to investigate PBAs are proposed, including monitoring of the electronic transition, discussion of the chemical disorder, or probing of the interaction between the alkali cations and the bimetallic network.

2. Experimental

The syntheses of K_0CoFe, $Cs_{0.7}CoFe$, Na_2CoFe, Rb_2CoFe and Cs_2CoFe have been already described elsewhere [12,14]. IR/THz measurements were carried out at the AILES beamline at synchrotron SOLEIL (France). The synchrotron was operating in the equal filling mode with 416 approximately equally filled and spaced electron bunches. The average storage beam electron current for the present result was 400 mA. The IR/THz experimental set-up has already been described elsewhere [15,16]. All THz measurements were performed in the transmission mode using a Bruker IFS 125 Fourier transform interferometer fitted with 6 μm Mylar/Si multilayer beam splitter and a liquid-helium-cooled Si bolometer detector, and operated at 1-cm^{-1} resolution. The MIR measurements exploited the interferometer fitted with a KBr beamsplitter combined with a MCT detector. The Fourier transform spectrometer was evacuated down to a 2×10^{-5} mbar pressure (to minimize residual H_2O and CO_2 absorption in the spectrometer). The liquid absorption cell used for these experiments was filled with sample powder dispersed in Nujol and held between two diamond windows. For the FIR spectra, the detector was fitted with a 200–600-cm^{-1} cold optical filter and the spectrometer with a 12.5-mm entrance aperture, but the SR effective source diameter results in beam diameter that fulfills the resolution criterion. All spectra result from the averaging of 400 scans measured with a mobile mirror speed of 2.5 $cm \cdot s^{-1}$. In order to measure the absorption spectra at well-controlled temperatures, the liquid cell was mounted on a cold head controller by a close cycle cryostat (pulse tube from CryoMech). This set-up allowed the sample temperature to be controlled within 1 K. The transmission spectra were obtained by dividing the signal (I) by the signal transmitted through pure Nujol (I_0). All IR spectra are presented in absorbance ($A = \ln(I/I_0)$) as a function of the incident wavenumbers ω.

3. Results and discussion

3.1. Description of PBAs

PBAs are coordination polymers obtained in aqueous solution from the substitution of the water molecules in $[M(OH_2)_6]^{k+}$ complexes by the isocyanide ligands from $[M'(CN)_6]^{j-}$ complexes (where M and M′ are transition metal ions). The resulting M–N≡C–M′ linkages form a face-centered cubic lattice [17] that may exhibit vacancies in $M'(CN)_6$ units (Fig. 1). In the vicinity of these vacancies, water molecules are coordinated to the M cations.

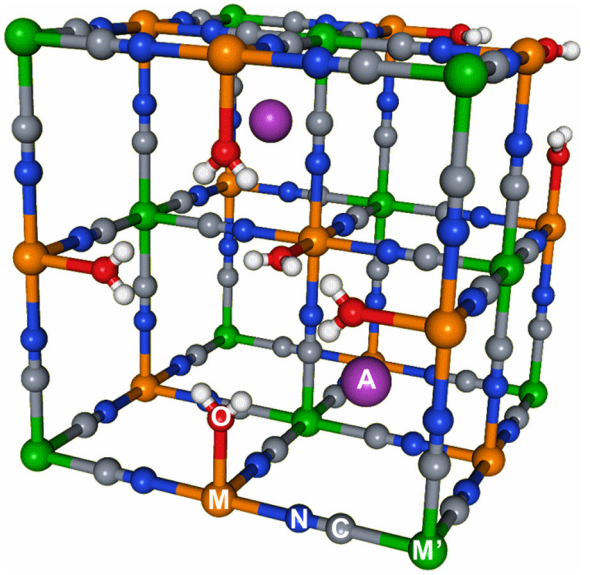

Fig. 1. Scheme of the unit cell of a Prussian blue analogue. Colors: M (orange), M′ (green), C (grey), N (blue), O (red), H (white), A (purple). For interpretation of references to color, see the online version of this article.

Additional alkali cations and zeolite water molecules can be inserted into the structure. The general formula of PBAs is $A_xM_4[M'(CN)_6]_{\alpha\square 4-\alpha} \cdot nH_2O$ (where A^+ is an alkali cation and □ is a $M'(CN)_6$ vacancy; $\alpha = 4(k + (x/4))/j$), called A_xMM' in the following. Depending on the nature of the A, M and M′ cations, the formers are known to interact with the bimetallic network in some PBAs [13].

The assignment of the IR vibration bands of PBAs has been performed thanks to a series of cobalt–iron PBAs (A_xCoFe) where $k = 2$ and $j = 3$. The general formula of A_xCoFe is therefore given by $A_xCo_4[Fe(CN)_6]_{(8+x)/4\square(4-x)/3} \cdot nH_2O$. Thus, the stoichiometry of A_xCoFe is completely defined by the amount x of alkali cations inserted in the structure. The A_xCoFe PBAs can exhibit two different $Co^{II}(HS)Fe^{III}(LS)$ and $Co^{III}(LS)Fe^{II}(LS)$ (HS: high spin; LS: low spin) electronic states [18] (called $Co^{II}Fe^{III}$ and $Co^{III}Fe^{II}$ in the following). However, as the amounts of cobalt and iron cations per unit cell are not the same, part of cobalt cations cannot undergo the $Co^{II}Fe^{III} \leftrightarrow Co^{III}Fe^{II}$ electronic transition. Consequently, the chemical formula of A_xCoFe PBAs can be rephrased as $A_xCo^{II}{}_4[Fe^{III}(CN)_6]_{(8+x)/3\square(4-x)/3} \cdot nH_2O$ (in the $Co^{II}Fe^{III}$ state) and $A_xCo^{III}{}_{(8+x)/3}Co^{II}{}_{(4-x)/3}[Fe^{II}(CN)_6]_{(8+x)/3\square(4-x)/3} \cdot nH_2O$ (in the $Co^{III}Fe^{II}$ state), taking into account the small amount of residual Co^{II} cations in the $Co^{III}Fe^{II}$ state.

According to the chemical composition and the structure of PBAs, their IR spectrum is expected to exhibit the following vibration bands:

- the ν{C≡N} vibration band, related to the cyanide bridges;
- the ν{M–N}, ν{M–O} and ν{M′–C} vibration bands, related to the metal-to-ligand bonds;
- the ν{O–H} vibration band, related to the water molecules of the system (both zeolite water molecules and water molecules bound to the M cations at the $M'(CN)_6$ vacancies).

3.2. Assignment of the ν{C≡N} vibration band

The ν{C≡N} vibration band is located in the 2100–2200-cm^{-1} spectral range. As the cyanide bridge is extremely sensitive to its environment, including the oxidation state and the spin state of the M and M′ cations, the ν{C≡N} band has already been extensively used to characterize the electronic state of switchable PBAs [19]. In the case of the A_xCoFe PBAs, the ν{C≡N} vibration band exhibits a maximum located at 2120 cm^{-1} in the $Co^{III}Fe^{II}$ state, characteristic of the cyanide bridge in the Co^{III}–N≡C–Fe^{II} linkages [19,20]. In the $Co^{II}Fe^{III}$ state, the maximum, located at 2160 cm^{-1}, is characteristic of the cyanide bridge in the Co^{II}–N≡C–Fe^{III} linkages [19,20]. The several minor contributions located between 2100 and 2120 cm^{-1} have been assigned to residual Co^{II}–N≡C–Fe^{II} linkages, surface non-bridging cyanides or residual Co^{III}–N≡C–Fe^{II} linkages [21]. The IR spectrum of the thermally switchable Na_2CoFe PBA [19,22] in both the $Co^{II}Fe^{III}$ and $Co^{III}Fe^{II}$ states is shown in Fig. 2. While the ν{C≡N} band shall contain a tremendous amount of information concerning PBAs (presence of minority species, interaction between the alkali cations and the bimetallic network, etc.), hardly obtainable through other techniques, the superimposition of several contributions for this vibration band over a very small spectral range results in a mutual hindering of this information. Consequently, the metal-to-ligand vibrations bands were investigated in order to unravel these various contributions to the electronic properties of PBAs.

3.3. Assignment of the ν{M–L} vibration bands

The assignment of the ν{M–L} vibration bands has been performed based on the $Co^{II}Fe^{III}$ ↔ $Co^{III}Fe^{II}$ thermally activated transition of Na_2CoFe [19,22] (Fig. 3). The IR spectrum of Na_2CoFe measured at different temperatures (200 K and 300 K) exhibits two pairs of vibration bands, coupled during the electronic transition, located respectively in the 150–350-cm^{-1} and 400–600-cm^{-1} spectral ranges. According to the literature dealing with the $[M(NH_3)_6]^{k+}$ (resp. $[M'(CN)_6]^{j-}$) complexes [23], the vibration bands in the 150–350-cm^{-1} (resp. 400–600 cm^{-1}) spectral range have been assigned to the Co–N (resp. Fe–C) bonds.

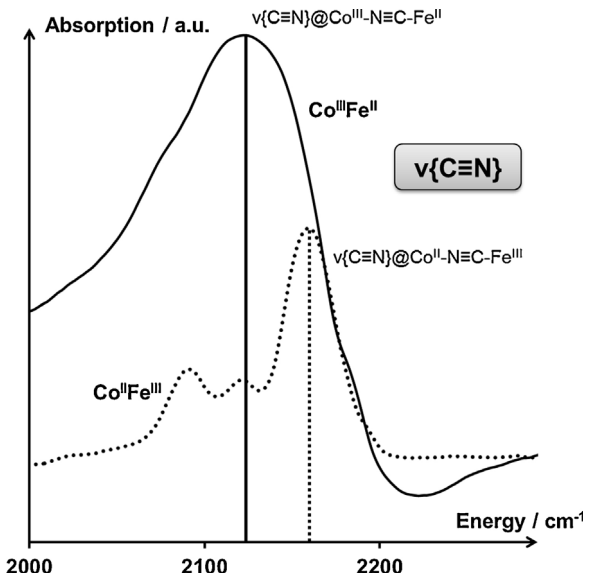

Fig. 2. Infrared spectrum of Na_2CoFe in the spectral range associated with the ν{C≡N} vibration band, both in the $Co^{II}Fe^{III}$ (T = 300 K) and $Co^{III}Fe^{II}$ (T = 200 K) electronic states. Assignments are detailed in the main text.

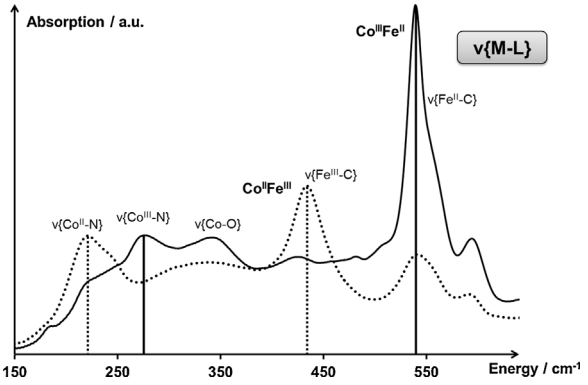

Fig. 3. Infrared spectrum of Na_2CoFe in the spectral range associated with the ν{M–L} vibration band, both in the $Co^{II}Fe^{III}$ (T = 300 K) and $Co^{III}Fe^{II}$ (T = 200 K) electronic states. Assignments are detailed in the main text.

Based on the $Co^{II}Fe^{III}$ electronic state of Na_2CoFe at T = 300 K, the band located at 220 cm^{-1} has been assigned to the Co^{II}–N bonds and the one located at 430 cm^{-1} has been assigned to the Fe^{III}–C bonds. Similarly, based on the $Co^{III}Fe^{II}$ electronic state of Na_2CoFe at T = 200 K, the band located at 270 cm^{-1} has been assigned to the Co^{III}–N bond and the band located at 540 cm^{-1} has been assigned to the Fe^{II}–C bond. Finally, the broad bands located in the 250–400 cm^{-1} spectral range have been assigned to the $Co^{II/III}$–O bonds, according to the literature dealing with the $[M(OH_2)_6]^{k+}$ complexes [23].

These assignments are in agreement with the vibration bands observed for the free $[M'(CN)_6]^{j-}$ complex [23]; for instance, the displacement of the ν{Fe^{II}–C} vibration band from 585 cm^{-1} in $[Fe(CN)_6]^{4-}$ to 540 cm^{-1} in the $Co^{III}Fe^{II}$ state of Na_2CoFe is consistent with the depletion of the electronic density on the $Fe(CN)_6$ entity due to the coordination of the isocyanide ligands to the cobalt cations [23].

3.4. Assignment of the ν{O–H} vibration bands

The spectral range associated with the ν{O–H} vibration band in PBAs comprises two distinct regions:

- from 3000 to 3500 cm^{-1}, the IR spectrum exhibits very broad bands associated with water molecules involved in a hydrogen-bonded network;
- from 3550 to 3700 cm^{-1}, the IR spectrum exhibits one or several very sharp bands associated with water molecules that are not involved in a hydrogen-bonded network.

The number of the sharp bands in the 3550–3700-cm^{-1} spectral range may vary depending on the nature of the

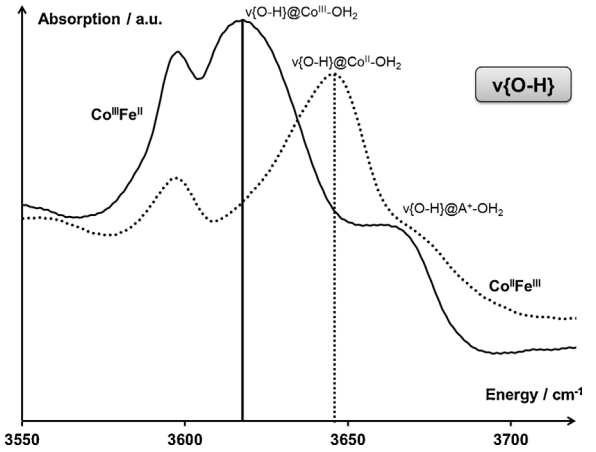

Fig. 4. Infrared spectrum of Na_2CoFe in the spectral range associated with the ν{O–H} vibration band of water molecules that are not involved in a hydrogen-bonded network, both in the $Co^{II}Fe^{III}$ ($T = 300$ K) and $Co^{III}Fe^{II}$ ($T = 200$ K) electronic states. Assignments are detailed in the main text.

PBA (supplementary data). According to their position in energy, comprised between 3590 cm^{-1} (water dimers [24]) and 3755 cm^{-1} (isolated water molecules [25]), the bands located in the 3600–3700 cm^{-1} range have been assigned to water molecules bound to metallic cations (either transition metal cations M or alkali cations A). This assignment can be further refined when considering the electronic transition of the Na_2CoFe PBA (Fig. 4).

Amongst the three vibration bands located in the 3600–3700-cm^{-1} range in Na_2CoFe, the two located at a lower energy are evolving through the $Co^{II}Fe^{III} \leftrightarrow Co^{III}Fe^{II}$ electronic transition. Consequently, these two bands have been assigned to water molecules bound to the cobalt cations at the $Fe(CN)_6$ vacancies. Based on the $Co^{II}Fe^{III}$ electronic state of Na_2CoFe at $T = 300$ K, the band located at 3645 cm^{-1} has been assigned to the ν{O–H} vibration of water molecules bound to Co^{II} cations; similarly, based on the $Co^{III}Fe^{II}$ electronic state of Na_2CoFe at $T = 200$ K, the band located at 3620 cm^{-1} has been assigned to the ν{O–H} vibration of water molecules bound to Co^{III} cations. This assignment is consistent with the water-to-bimetallic network partial charge transfer relying on the mostly σ character of the water-to-metal bond: in the $Co^{II}Fe^{III}$ electronic state, the depletion of the electronic density on a water molecule bound to the Co^{II} cation is rather small, which results in a rather strong O–H bond (ν{O–H} = 3645 cm^{-1}); in the $Co^{III}Fe^{II}$ electronic state, the depletion of the electronic density on a water molecule bound to the Co^{III} cation is much more important, which results in a weaker O–H bond (ν{O–H} = 3620 cm^{-1}).

The higher energy band has been assigned to water molecules bound to alkali cations. The appearance and the intensity of this latter vibration band are highly sensitive to the nature and the amount of alkali cations per unit cell (supplementary data).

This assignment of the IR spectrum of PBAs over the whole 100–4000-cm^{-1} spectral range allows the fine investigation of the structure of PBAs (presence of vacancies, position of the alkali cation in the lattice, etc.) and the alkali-cyanide interaction [13]. The following sections aim at demonstrating the relevance of the IR spectroscopy in the study of such properties of PBAs, which cannot be probed by other techniques.

3.5. Signatures of the $M'(CN)_6$ vacancies

In the $Co^{II}Fe^{III}$ electronic state, the chemical formula of A_xCoFe PBAs can be rephrased as $A_xCo^{II}_4[Fe^{III}(CN)_6]_{(8+x)/3}\square_{(4-x)/3}\cdot nH_2O$. Consequently, the mean composition of the coordination sphere of the Fe^{III} cations is always given by $Fe^{III}(C{\equiv}N{-}Co^{II})_6$, whatever the amount x of alkali cations inserted in the structure. A single type of $\nu\{Fe^{III}{-}C\}$ vibration band, associated with the $Co^{II}{-}N{\equiv}C{-}Fe^{III}$ linkages, is therefore expected for the A_xCoFe PBAs in the $Co^{II}Fe^{III}$ electronic state.

The IR spectrum of the A_xCoFe PBAs in the $Co^{II}Fe^{III}$ electronic state in the spectral range associated with the $\nu\{Fe^{III}{-}C\}$ vibration band shows a single contribution, whichever the nature and the amount x of inserted alkali cations (Fig. 5). This observation is consistent with the expected single contribution to this band for the A_xCoFe PBAs in the $Co^{II}Fe^{III}$ electronic state.

The situation is however very different for the $Co^{III}Fe^{II}$ electronic state: according to the $A_xCo^{III}_{(8+x)/3}Co^{II}_{(4-x)/3}[Fe^{II}(CN)_6]_{(8+x)/3}\square_{(4-x)/3}\cdot nH_2O$ chemical formula of the A_xCoFe PBAs in the $Co^{III}Fe^{II}$ state, each octahedral Fe^{II} cation exhibits a mean $Fe^{II}(C{\equiv}N{-}Co^{III})_{(8+x)/2}(C{\equiv}N{-}Co^{II})_{(4-x)/2}$ coordination sphere. While the presence of residual Co^{II} cations can be monitored by magnetic measurements, the subsequent $Co^{II}{-}N{\equiv}C{-}Fe^{II}$ linkages are hardly measurable by IR spectroscopy in the ν{C≡N} spectral range due to:

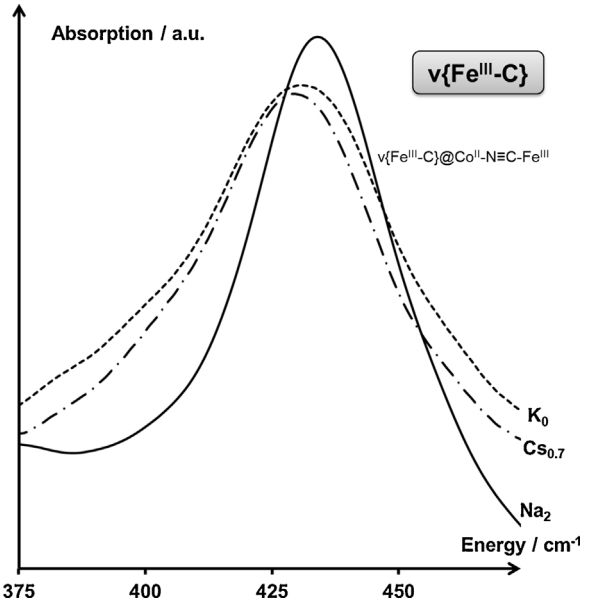

Fig. 5. Infrared spectrum of the K_0CoFe (—), $Cs_{0.7}CoFe$ (—·—), Na_2CoFe (—) PBAs in the $Co^{II}Fe^{III}$ electronic state, in the spectral range associated with the $\nu\{Fe^{III}{-}C\}$ vibration band, at $T = 300$ K. Assignments are detailed in the main text.

- the small amount of these Co^{II}–N≡C–Fe^{II} linkages in $Co^{III}Fe^{II}$ PBAs;
- the superimposition of numerous contributions to the IR spectrum in the ν{C≡N} region.

In Na_2CoFe ($x = 2$), the mean coordination sphere of the iron cations depends on the electronic state of the system: in the $Co^{II}Fe^{III}$ state, the mean coordination sphere of Fe^{III} is $Fe^{III}(C{\equiv}N{-}Co^{II})_6$, while in the $Co^{III}Fe^{II}$ state, the mean coordination sphere of Fe^{II} is $Fe^{II}(C{\equiv}N{-}Co^{III})_5(C{\equiv}N{-}Co^{II})_1$. In the $Co^{II}Fe^{III}$ state, the IR spectrum of Na_2CoFe (Fig. 6a) exhibits a single symmetrical band ($\nu\{Fe^{III}{-}C\} = 433\ cm^{-1}$); in the $Co^{III}Fe^{II}$ state, the IR spectrum of Na_2CoFe (Fig. 6b) exhibits a well-defined main contribution ($\nu\{Fe^{II}{-}C\} = 539\ cm^{-1}$) and a broad shoulder at higher energy. These observations are consistent with the anticipated coordination spheres for the iron cations: the single contribution to the ν{Fe^{III}–C} vibration band can be assigned to the Fe^{III}–C bond in Co^{II}–N≡C–Fe^{III} linkages; the two contributions to the ν{Fe^{II}–C} vibration band can be assigned to the Fe^{II}–C bonds in Co^{III}–N≡C–Fe^{II} and Co^{II}–N≡C–Fe^{II} linkages. According to:

- the relative intensity of the two contributions to the ν{Fe^{II}–C} vibration band;
- the broadness of the contribution at higher energy, the main contribution has been assigned to the Fe^{II}–C in the majority Co^{III}–N≡C–Fe^{II} linkages, while the higher energy contribution has been assigned to the Fe^{II}–C in the minority Co^{II}–N≡C–Fe^{II} linkages.

The broad width of the higher energy shoulder is consistent with the mismatch between the Co^{II}–N≡C–Fe^{II} linkage and the surrounding mostly $Co^{III}Fe^{II}$ environment, resulting in some structural disorder.

This study highlights the relevance of the IR spectroscopy in the investigation of the different Co–N≡C–Fe linkages in A_xCoFe PBAs.

3.6. Study of the alkali–cyanide interaction

The existence of an interaction between the alkali cations and the bimetallic network has already been evidenced in some A_xCoFe PBAs [13]. This interaction, whose nature is still debated, may result in the modulation of the relative stability of the $Co^{II}Fe^{III}$ and $Co^{III}Fe^{II}$ electronic states, as evidenced, for instance, in the A_2CoFe series: while the Rb_2CoFe and Cs_2CoFe PBAs always exhibit a $Co^{III}Fe^{II}$ ground state [26], Na_2CoFe shows a thermal transition between the $Co^{II}Fe^{III}$ and $Co^{III}Fe^{II}$ states around T = 250 K [19,22]. According to the nucleophilic nature of the cyanide bridge, the interaction between the alkali cations and the bimetallic network is expected to involve the electron-rich bridging cyanide ligands. However, no direct signature of this interaction has been, to date, proposed in the literature.

In the A_2CoFe series of PBAs, all the compounds exhibit the same $\{Co_4[Fe(CN)_6]_{3.3\square 0.7}(OH_2)_4\}$ bimetallic network. In the $Co^{III}Fe^{II}$ state, the cobalt cations of these PBAs share a common $Co^{III}(N{\equiv}C{-}Fe^{II})_5(OH_2)_1$ mean coordination sphere. The IR spectra of Rb_2CoFe and Cs_2CoFe in the $Co^{III}Fe^{II}$ state (Fig. 7) exhibit a single contribution to the ν{Co^{III}–N} vibration band, which has therefore been assigned to the Co^{III}–N in the Co^{III}–N≡C–Fe^{II} linkages. However, the IR spectrum of Na_2CoFe in the $Co^{III}Fe^{II}$ state (Fig. 7) shows two distinct contributions for the ν{Co^{III}–N} vibration band. The nature of the alkali cation being the sole difference between these A_2CoFe PBAs, this splitting of the ν{Co^{III}–N} vibration band is therefore due to the different interactions between the alkali cations and the bimetallic network.

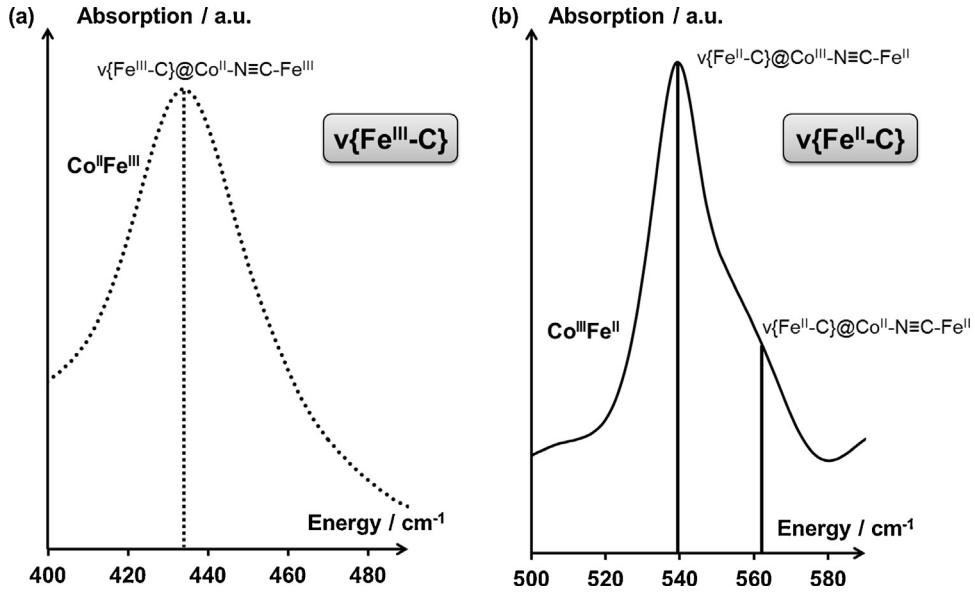

Fig. 6. Infrared spectrum of Na_2CoFe in the spectral range associated with the ν{Fe–C} vibration band, (a) in the $Co^{II}Fe^{III}$ ($T = 300$ K) electronic state and, (b) in the $Co^{III}Fe^{II}$ ($T = 200$ K) electronic state. Assignments are detailed in the main text.

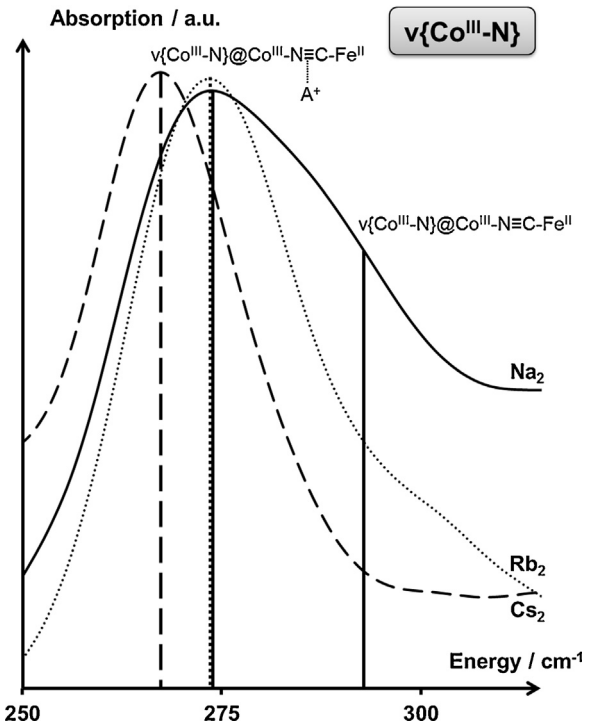

Fig. 7. Infrared spectrum of the Na_2CoFe (—), Rb_2CoFe (•••) and Cs_2CoFe (— — —) PBAs in the $Co^{III}Fe^{II}$ state ($T = 200$ K) in the $\nu\{Co^{III}–N\}$ spectral range. Assignments are detailed in the main text.

The presence of two contributions for the $\nu\{Co^{III}–N\}$ vibration band in Na_2CoFe reveals two chemically non-equivalent Co^{III}–N bonds, which have been assigned to Co^{III}–N≡C–Fe^{II} linkages interacting and non-interacting with an alkali cation [11]. Thus, the difference in energy between these two contributions is a probe of the strength of the alkali–cyanide interaction.

This assignment can be further confirmed by considering the Cs_xCoFe series of PBAs. In the case of large alkali cations standing at the center of the octants of the lattice (Fig. 1), each alkali cation can interact with a maximum of 12 cyanide bridges. In a given A_xCoFe series, each unit cell comprises $2 \times (8 + x)$ cyanide bridges; therefore a maximum of $2x \times (8 + x)$ cyanide bridges per unit cell are interacting with an alkali cation. Consequently, if $x \geq 1$, each cyanide bridge is interacting with an alkali cation, and the resulting $\nu\{Co–N\}$ vibration band should exhibit a single contribution. On the contrary, in the case of A_xCoFe PBAs with low amounts of alkali cations per unit cell ($x < 1$), two contributions are expected for the $\nu\{Co–N\}$ vibration band, one corresponding to the Co–N in Co–N≡C–Fe linkages that are not interacting with an alkali cation, and the other corresponding to Co–N≡C–Fe linkages interacting with an alkali cation. Such assumption can be confirmed in the Cs_xCoFe series: while the $Cs_{0.7}CoFe$ PBA ($x < 1$) shows a splitting of the $\nu\{Co^{II}–N\}$ vibration band in the $Co^{II}Fe^{III}$ electronic state (Fig. 8), no splitting of the $\nu\{Co^{III}–N\}$ vibration band is observed in the $Co^{III}Fe^{II}$ electronic state of Cs_2CoFe ($x \geq 1$) (Fig. 7). Furthermore, no splitting of the $\nu\{Co^{II}–N\}$ vibration band is observed in the case of the alkali-free K_0CoFe PBA (Fig. 8).

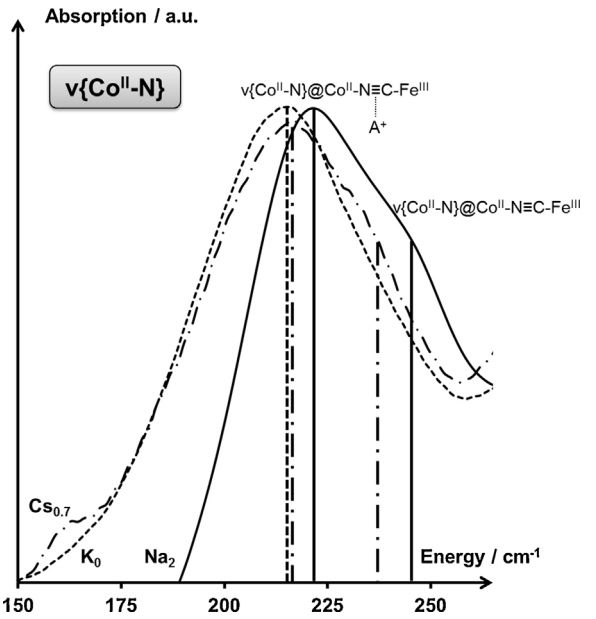

Fig. 8. Infrared spectrum of the K_0CoFe (—), $Cs_{0.7}CoFe$ (—·—) and Na_2CoFe (—) Prussian blue analogues in the $Co^{II}Fe^{III}$ state ($T = 300$ K) in the spectral range associated with the $\nu\{Co^{II}–N\}$ vibration band. Assignments are detailed in the main text.

3.7. Positioning of the alkali cation

IR study of the alkali-cyanide interaction taking place in A_xCoFe PBAs can also bring some insight into the much debated question of the position of the alkali cation in the lattice. While the initial description of PBAs locates the alkali cations at the center of the octants of the lattice [17], recent studies tend to question this positioning [11,27]. Indeed, according to the distance between the center of the octants and the cyanide bridges, this positioning seems unsuitable for smaller alkali cations. Consequently, in the case of small alkali cations, a splitting of the $\nu\{Co–N\}$ vibration band is anticipated even for A_xCoFe PBAs with an important amount of alkali cations per unit cell. Experimentally, two distinct contributions to the $\nu\{Co–N\}$ vibration band are observed for the Na_2CoFe PBA, for which both the $\nu\{Co^{II}–N\}$ vibration band (in the $Co^{II}Fe^{III}$ electronic state; Fig. 8) and the $\nu\{Co^{III}–N\}$ vibration band (in the $Co^{III}Fe^{II}$ electronic state; Fig. 7), corresponding to the Co–N bonds implied either in the Co–N≡C–Fe linkages interacting with an alkali cation, or in the Co–N≡C–Fe linkages that are not interacting with an alkali cation. This splitting of the $\nu\{Co–N\}$ vibration band in Na_2CoFe indicates that the sodium cation does not stand at the center of the octants of the lattice. Such results demonstrate that IR spectroscopy can bring new insights into the intimate structure of PBAs, as such information cannot be inferred from standard X-ray diffraction studies of PBAs containing small, disordered alkali cations. Further refinement of the position(s) of the alkali cations in the unit cell of PBAs and highlighting of possible displacements of the alkali cations in the unit cell are in progress.

Finally, the impact of the interaction between the alkali cation and the bimetallic network on the metal–ligand

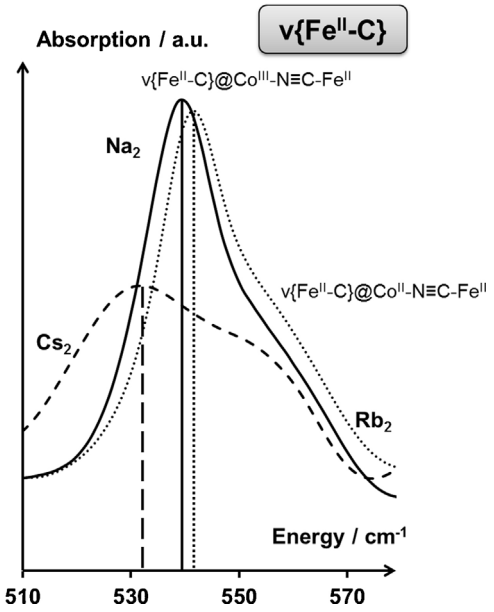

Fig. 9. Infrared spectrum of the Na_2CoFe (—), Rb_2CoFe (•••) and Cs_2CoFe (— — —) Prussian blue analogues in the $Co^{III}Fe^{II}$ state ($T = 200$ K) in the $\nu\{Fe^{II}–C\}$. Assignments are detailed in the main text.

bonds can also be pointed out in the Cs_2CoFe PBA: while no splitting of the $\nu\{Co^{III}–N\}$ vibration band is observed for this system in the $Co^{III}Fe^{II}$ state (Fig. 7), a broadening of the contributions to the $\nu\{Fe^{II}–C\}$ vibration band is evidenced. This broadening reveals a perturbation of the $Fe(CN)_6$ units due to the presence of the large cesium cations, with respect to smaller ones (as rubidium cations; Fig. 9).

This last series of examples highlights the suitability of IR spectroscopy to the fine investigation of the weak interactions between the alkali cation and the bimetallic network in PBAs, hardly detectable at the macroscopic scale, taking place in PBAs.

4. Conclusion

The investigation by IR spectroscopy of switchable PBAs allowed the comprehensive assignment of the IR spectrum of PBAs over the whole 150–4000 cm^{-1} spectral range, including vibration bands associated with metal–ligand bonds, cyanide bridges and water molecules that are not involved in a network of hydrogen bonds. The existence of minority species, such as $Co^{II}–N\equiv C–Fe^{II}$ linkages in A_xCoFe PBAs, has been pointed out. Direct evidences of the interaction between the inserted alkali cations and the bimetallic network taking place in PBAs have been demonstrated, paving the way to the study of the position of the alkali cation within the lattice of PBAs. This work constitutes a milestone in the study of PBAs and related molecular compounds by providing a reliable reference for the comprehensive assignment of the IR spectrum of such systems.

Appendix A. Supplementary data

Supplementary data associated with this article can be found, in the online version, at http://dx.doi.org/10.1016/j.crci.2014.01.017.

References

[1] T. Mallah, S. Thiébaut, M. Verdaguer, P. Veillet, Science 262 (1993) 1554.
[2] S. Ferlay, T. Mallah, R. Ouahès, P. Veillet, M. Verdaguer, Nature 378 (1995) 701.
[3] M.R. Hartman, V.K. Peterson, Y. Liu, S.S. Kaye, J.R. Long, Chem. Mater. 18 (2006) 3221.
[4] J. Jiménez-Gallegos, J. Rodríguez-Hernández, H. Yee-Madeira, E. Reguera, J. Phys. Chem. C 114 (2010) 5043.
[5] P.K. Thallapally, R.K. Motkuri, C.A. Fernandez, B.P. McGrail, G.S. Behrooz, Inorg. Chem. 49 (2010) 4909.
[6] D. Asakura, C.H. Li, Y. Mizuno, M. Okubo, H. Zhou, D.R. Talham, J. Am. Chem. Soc. 135 (2013) 2793.
[7] Y. Lu, L. Wang, J. Cheng, J.B. Goodenough, Chem. Commun. 48 (2012) 6544.
[8] O. Sato, T. Iyoda, A. Fujishima, K. Hashimoto, Science 272 (1996) 704.
[9] Y. Moritomo, M. Hanawa, Y. Ohishi, K. Kato, M. Takata, A. Kuriki, E. Nishibori, M. Sakata, S. Ohkoshi, H. Tokoro, K. Hashimoto, Phys. Rev. B: Condens. Matter 68 (2003) 144106.
[10] J.-D. Cafun, J. Lejeune, F. Baudelet, P. Dumas, J.-P. Itié, A. Bleuzen, Angew. Chem. Int. Ed. 51 (2012) 9146.
[11] J. Lejeune, J.-D. Cafun, G. Fornasieri, J.-B. Brubach, G. Creff, P. Roy, A. Bleuzen, Eur. J. Inorg. Chem. 2012 (2012) 3980.
[12] A. Bleuzen, V. Escax, J.-P. Itié, P. Münsch, M. Verdaguer, C.R. Chimie 6 (2003) 343.
[13] J.-D. Cafun, G. Champion, M.A. Arrio, C. Cartier dit Moulin, A. Bleuzen, J. Am. Chem. Soc. 132 (2010) 11552.
[14] A. Bleuzen, C. Lomenech, V. Escax, F. Villain, F. Varret, C. Cartier dit Moulin, M. Verdaguer, J. Am. Chem. Soc. 122 (2000) 6648.
[15] J.-B. Brubach, L. Manceron, M. Rouzieres, O. Pirali, D. Balcon, F.K. Tchana, V. Boudon, M. Tudorie, T. Huet, A. Cuisset, P. Roy, AIP Conf. Proc. 1214 (2010) 81.
[16] P. Roy, M. Rouzières, Z. Qi, O. Chubar, Infrared Phys. Technol. 49 (2006) 139.
[17] A. Ludi, H.U. Güdel, Inorg. Chem. 14 (1973) 1.
[18] T. Yokoyama, M. Kiguchi, T. Ohta, O. Sato, Y. Einaga, K. Hashimoto, Phys. Rev. B: Condens. Matter 60 (1999) 9340.
[19] N. Shimamoto, S.I. Ohkoshi, O. Sato, K. Hashimoto, Inorg. Chem. 41 (2002) 678.
[20] R.O. Lezna, R. Romagnoli, N.R. de Tacconi, K. Rajeshwar, J. Phys. Chem. B 106 (2002) 3612.
[21] O. Sato, Y. Einaga, A. Fujishima, K. Hashimoto, Inorg. Chem. 38 (1999) 4405.
[22] R. Le Bris, J.-D. Cafun, C. Mathonière, A. Bleuzen, J.-F. Létard, New J. Chem. 33 (2009) 1255.
[23] K. Nakamoto, Infrared and Raman Spectra of Inorganic and Coordination Compounds, John Wiley & Sons, Inc. Hoboken, New Jersey, 2008, p. 1.
[24] J. Ceponkus, P. Uvdal, B. Nelander, J. Phys. Chem. A 112 (2008) 3921.
[25] B.T. Darling, D.M. Dennison, Phys. Rev. 57 (1940) 128.
[26] V. Escax, A. Bleuzen, C. Cartier dit Moulin, F. Villain, A. Goujon, F. Varret, M. Verdaguer, J. Am. Chem. Soc. 123 (2001) 12536.
[27] A. Bleuzen, V. Escax, A. Ferrier, F. Villain, M. Verdaguer, P. Münsch, J.-P. Itié, Angew. Chem. Int. Ed. 43 (2004) 3728.